Discover Oncology

Research

Nebulized inhalation of extracellular vesicles containing SPOCK2 suppresses lung adenocarcinoma progression via MAPK inhibition

Ying Wang[1,2] · Ningning Liu[2] · Chuanqin Xu[2] · Jing Wang[2] · Liyang Dong[3] · Shuang Yang[1,4] · Junhong Jiang[1]

Received: 15 November 2024 / Accepted: 8 May 2025
Published online: 17 May 2025

Abstract
Aberrant expression of SPARC/osteonectin, cwcv and kazal-like domains proteoglycan 2 (SPOCK2) plays a role in the development and progression of several human cancers. However, the importance of its expression and function in lung adenocarcinoma (LUAD) remains unclear. The present study aimed to elucidate the role of SPOCK2 in the growth of LUAD and propose a novel therapeutic insight for LUAD through SPOCK2. SPOCK2 protein expression was significantly reduced in LUAD tissues and cells by Immunohistochemical assay and Western blot. CCK-8, colony formation, and Transwell assays were used to demonstrate that SPOCK2 overexpression inhibited both proliferation and migration of LUAD cells in vitro. This inhibition of tumor growth was further confirmed by a LUAD xenograft mouse model in vivo. To explore downstream target signal of SPOCK2 in LUAD, RNA transcriptome sequencing was performed and enrichment analysis showed an association between SPOCK2 expression and the MAPK pathway. Furthermore, HEK293T cells were modified with SPOCK2, and extracellular vesicles (EVs) containing SPOCK2 (SPOCK2-EVs) were collected through ultra-high-speed centrifugation. Interestingly, co-culture with SPOCK2-EVs significantly increased SPOCK2 levels within LUAD cells. Furthermore, SPOCK2-EVs effectively inhibited LUAD growth in vitro and in vivo studies. Because directly injecting SPOCK2-EVs into tumors presents challenges for internal organs, we investigated the efficacy of nebulized SPOCK2-EVs for LUAD treatment. Consistent with our findings from intratumoral injection, nebulized inhalation of SPOCK2-EVs resulted in significant inhibition of LUAD growth. These results strongly suggest that SPOCK2 released by HEK293T-EVs can effectively inhibit LUAD tumor growth and hold promise for future clinical translation in cancer therapy.

Keywords SPOCK2 · MAPK · Extracellular vesicles · Lung adenocarcinoma · Nebulized inhalation

Supplementary Information The online version contains supplementary material available at https://doi.org/10.1007/s12672-025-02626-9.

✉ Liyang Dong, liyangdong@ujs.edu.cn; ✉ Shuang Yang, yangs2020@suda.edu.cn; ✉ Junhong Jiang, jiangjunhong1969@suda.edu.cn; Ying Wang, wangying_wyy@126.com; Ningning Liu, 285449096@qq.com; Chuanqin Xu, 657442476@qq.com; Jing Wang, 1937174876@qq.com | [1]Department of Pulmonary and Critical Care Medicine, The Fourth Affiliated Hospital of Soochow University, No. 9 Chongwen Road, Suzhou Industrial Park, Suzhou 215123, Jiangsu, People's Republic of China. [2]Department of Respiratory Diseases, The Affiliated Huai'an Hospital of Xuzhou Medical University, Huai'an 223002, Jiangsu, People's Republic of China. [3]Department of Nuclear Medicine, The Affiliated Hospital of Jiangsu University, No. 438 Jiefang Road, Jingkou District, Zhenjiang 212000, Jiangsu, People's Republic of China. [4]Center for Clinical Mass Spectrometry, College of Pharmaceutical Sciences, Soochow University, Suzhou 215123, Jiangsu, People's Republic of China.

1 Introduction

Lung cancer is a leading cause of morbidity and mortality worldwide, with two main types: small cell lung cancer (SCLC) and non-small cell lung cancer (NSCLC) [1]. NSCLC, accounting for 85–90% of all lung cancers, is further classified into lung adenocarcinoma (LUAD), squamous lung cancer, and large cell lung cancer, with LUAD being the most prevalent subtype at over 40% [2]. Despite advancements in targeted therapies, the 5-year survival rate for LUAD patients remains below 20% [3, 4]. Even after surgery, the current mainstay of treatment, 30% of stage I LUAD patients experience recurrence or metastasis within five years [5]. This highlights the urgent need for a deeper understanding of LUAD's molecular mechanisms and the development of novel therapeutic approaches.

SPOCK family proteins are proteoglycans found in the vertebrate extracellular matrix (ECM) [6]. This family consists of three members: SPOCK1, SPOCK2, and SPOCK3 [7]. SPOCK-encoded proteins play various roles in health and disease, including tumor progression [8], epithelial-mesenchymal transition [9], and Alzheimer's disease [10]. SPOCK2 (SPARC (osteonectin), cwcv and kazal-like domains proteoglycan 2), also known as testican-2, is a member of the SPOCK family synthesized by lung epithelial cells and fibroblasts. It plays a significant role in cancer cell behavior [7]. Notably, SPOCK2 exhibits opposing effects in different cancers, inhibiting tumor growth in pancreatic, endometrial, and prostate cancers [7, 11, 12], while promoting it in ovarian cancer [13]. In LUAD, bioinformatics analyses revealed downregulation of SPOCK2 compared to normal lung tissue, with a correlation to immune infiltration [14]. Additionally, a recent study suggests that EZH2 suppresses LUAD growth by acting through SPOCK2 and SPRED1 [15]. These findings suggest SPOCK2 as a key molecule in LUAD development, warranting further investigation.

Our findings demonstrate significantly reduced SPOCK2 levels in both LUAD tissues and cells. SPOCK2 overexpression inhibited LUAD cell proliferation and migration, likely through inactivation of the MAPK signaling pathway. HEK293T cells were transfected with SPOCK2-overexpressing lentivirus to generate SPOCK2-EVs. Both in vitro and in vivo experiments demonstrated that SPOCK2-EVs suppress the growth of LUAD. In conclusion, this study reveals a dual inhibitory role for SPOCK2 in LUAD: directly suppressing cell proliferation and migration via the MAPK pathway, and potentially serving as a therapeutic candidate delivered through EVs.

2 Materials and methods

2.1 Human lung tissue samples

LUAD and normal lung tissue specimens were obtained from surgical resections at the Affiliated Huai'an Hospital of Xuzhou Medical University (Huai'an, China). Patients who had received preoperative radiotherapy or chemotherapy were excluded. All participants or their guardians provided written informed consent form before enrollment. The study was conducted in accordance with the principles of the Declaration of Helsinki, and the protocol was approved by the Ethics Committee of the Affiliated Huai'an Hospital of Xuzhou Medical University.

2.2 Cell culture

A549, H1944, CL1-0, and CL1-5 cell lines were purchased from Cell Bank of Chinese Academy of Sciences and cultured in 1640 medium (Gibco, Carlsbad, CA) containing 10% FBS (Gibco) and 1% pen/strep (Gibco) at 37 °C and 5% CO_2. Normal human bronchial epithelial cells BEAS-2B and HEK293T were purchased from the American Type Culture Collection (Manassas, VA) and were cultured in DMEM (Gibco, Carlsbad, CA) with the addition of 10% FBS and 1% pen/strep in 5% CO_2 and 37 °C. A549-LUC was purchased from Shanghai Fuheng Biotechnology Co., Ltd and cultured in F-12K (Fuheng, Shanghai, China) with the addition of 10% FBS and 1% pen/strep in 5% CO_2 and 37 °C.

2.3 Lentivirus transduction

Lentiviral particles for SPOCK2 overexpression (LV-SPOCK2) and its control (LV-NC) were packaged and purchased from GeneChem (Shanghai, China). When cell confluency reaches 50–60%, transfect LV-SPOCK2 and LV-NC lentivirus

in 6-well plates according to the manufacturer's instructions. After 12 h, carefully remove the supernatant containing lentivirus and replace it with fresh complete medium.

2.4 Databases usage

The UALCAN database (http://ualcan.path.uab.edu/index.html) is an interactive web-based tool that provides information on gene expression, survival analysis, and epigenetic modifications [16]. In the TCGA module, after the input of the target gene SPOCK2 and the target tumor LUAD, the expression of SPOCK2 in LUAD based on sample types was online. The GEPIA (http://gepia.cancer-pku.cn/) database is used for gene expression analysis, survival analysis, similar gene prediction, and more [17]. We used this database to analyze the overall survival correlation of SPOCK2 expression. Click "Survival", enter the target gene SPOCK2 and LUAD, then the overall survival plot will be generated online.

2.5 Extraction and characterization of extracellular vesicles

EVs were isolated from the supernatant of both overexpressed-SPOCK2 HEK293T and control-SPOCK2 HEK293T cells using ultra-high-speed centrifugation (Beckman Coulter Optima L-100 XP ultracentrifuge). The cells were initially incubated with DMEM containing 10% FBS in cell culture dishes to reach approximately 70% confluency. The medium was then replaced with serum-free DMEM for 24 h. The cell supernatants were collected and centrifuged at 300×*g* for 10 min, 2000×*g* for 20 min to discard cell debris. EVs were isolated by ultracentrifugation (Beckman Coulter Optima L-100 XP ultracentrifuge) at 100,000×*g* for 90 min. The supernatant was then removed, and the remaining precipitate contained the EVs. Next, the EVs were resuspended by adding PBS and stored at −80 °C until needed. The protein concentration of EVs was determined by BCA protein assay kit (Beyotime, Nantong, China). EV surface markers HSP70 (ab181606, Abcam, Cambridge, MA), and TSG101 (ab133586, Abcam) were detected by Western blot (WB). Shape of EVs was observed using transmission electron microscopy (JEM-1200EX; JEOL Ltd., Tokyo, Japan). The particle size distribution of EVs was determined by nanoparticle trafficking analysis using ZetaView PMX 110 (Particle Metrix, Meerbusch, Germany) according to the manufacturer's protocols.

2.6 RNA sequencing

Total RNA was extracted from control and LV-SPOCK2 of A549 cells using mirVana RNA isolation kit (Ambion, Austin, TX) according to the manufacturer's manual. Then we evaluate RNA integrity using Agilent Bioanalyzer 2100 (Agilent, Santa Clara, CA). RNA sequencing experiment was conducted by LC-BIO Bio Technology (Hangzhou, China). After sequencing, the data ($|\log FC| > 1$ and adjusted $P < 0.05$) were further analyzed on the free online platform of LC-Bio Cloud Platform (https://www.omicstudio.cn/).

2.7 Protein extraction and western blotting

The proteins were extracted from cells and EVs with RIPA buffer (Cell Signaling Technology Inc., Danvers, MA) and quantified with a BCA Protein Kit (Beyotime). 30 ug protein sample was separated by 10% SDS-PAGE, transferred to polyvinylidene difluoride (PVDF) membranes (Bio-Rad) and then incubated with primary antibody at 4 °C overnight. The antibodies to SPOCK2 (ab217044), Erk1/2 (ab17942), p-Erk1/2 (ab201015), HSP70 (ab181606), Tsg101 (ab133586) were all purchased from Abcam; β-actin, HRP-labeled goat anti-rabbit/mouse IgG (H + L) were purchased from Beyotime (China). Following incubation with the secondary antibody for 1 h at 37 °C, target proteins were visualized on the PVDF membranes using a Pierce ECL kit. Images were captured using a DNR Bio Imaging System (Jerusalem, Israel).

2.8 Cell proliferation assay

Cell viability was determined by the CCK-8 assay (KeyGEN BioTECH, Nanjing, China), following the protocol provided by the manufacturer. Briefly, LUAD cells were inoculated in 96-well plates (2×10^3 cells/well). After the designated incubation periods (24, 48, 72, and 96 h), CCK-8 solution (10 µL) was added to each well, followed by a 2-h incubation. Absorbance was then measured at 450 nm using a microplate reader (Synergy HT, BioTek, Biotek Winooski, VT).

For the colony formation assay, A549 and H1944 cells were transfected with lentiviruses or treated with EVs. One thousand cells per well were then seeded into 6-well plates and cultured in medium containing 10% FBS. After 10 days,

the cells were fixed with methanol, stained with 0.4% crystal violet solution, and finally photographed. Colonies with over 50 cells were counted.

2.9 Cell migration assay

LUAD cells were cultured into the upper chamber of the Transwell (A549: 5×10^4; H1944: 4×10^4 in 200 µL serum-free medium). 600 µL of medium supplemented with 10% FBS was added to the lower chamber. After a 12-h incubation, cells remaining on the upper surface of the membrane were removed. The membrane was then fixed with methanol, stained with 0.4% crystal violet solution, and imaged using a Nikon microscope.

2.10 LUAD nude mouse subcutaneous tumor model

Four-week-old female BALB/c nude mice were purchased from the Center for Comparative Medicine, Yangzhou University (Yangzhou, China). To assess the effect of SPOCK2 on LUAD growth, A549 cells stably transfected with LV-SPOCK2 or NC-SPOCK2 (2×10^6 cells) were injected subcutaneously into the left or right abdomen of mice, respectively. To investigate the effect of SPOCK2-EVs on LUAD growth, nude mice were injected subcutaneously with A549 cells (2×10^6 cells) in the right abdomen. After 7-day tumor growth, PBS (20 µL), NC-EVs, or SPOCK2-EVs (all EVs: 2×10^{10} in a volume of 20 µL of PBS) were injected weekly into the tumors according to Bruno et al. [18, 19]. On day 28, the tumors were removed for examination. Tumor volume (mm^3) was calculated based on the length (L) and width (w) axis of the tumor according to the following formula: $V = L \times W^2/2$. In accordance with the protocols established by the Ethics Committee of Soochow University (SUDA20230428A06), the tumor size in animal experiments must be maintained below 2000 mm^3, and the tumor weight must not exceed 10% of the experimental animals' normal body weight during the investigation. Our research strictly adhered to these ethical requirements.

2.11 LUAD nude mouse in situ tumor formation model

To establish lung tumors in mice, a 5 mm incision is made approximately 1.5 cm above the left axillary anterior costal arch in four-week-old female BALB/c nude mice. The skin and subcutaneous tissue are carefully separated to expose the chest wall, allowing visualization of the lung lobes moving with respiration. Next, 2×10^6 A549-LUC cells are resuspended in 50 µL of PBS and mixed thoroughly with another 50 µL of Matrigel. This cell suspension is then injected into the left lung lobe using a 1 mL syringe with the needle inserted to a depth of about 3 mm. After pausing the injection for a few seconds, the needle is removed, and the incision is closed with sutures.

To evaluate the effect of nebulized inhalation of SPOCK2-EVs on LUAD growth, nude mice with in situ LUAD were inhaled with NC-EVs or SPOCK2-EVs (all EVs: 2×10^{10} in a volume of 0.5 mL of PBS) weekly. Four weeks later, D-luciferin potassium salt (Proteinbio, Nanjing, China) dissolved with sterile D-PBS (without $Mg^{2+}$and Ca^{2+}) was intraperitoneally injected at a dose of 150 mg/kg per mouse. Bioluminescence was measured by imaging mice anesthetized with isoflurane using the VILBER Fusion FX7 Imaging System. Images representing light intensity were generated, with blue corresponding to the lowest intensity and red signifying the highest. Following the study's conclusion, the mice were euthanized. Lungs were then harvested, and bioluminescence was measured by imaging the lungs with the VILBER Fusion FX7 Imaging System.

2.12 Immunohistochemical (IHC) assay

Specimens were fixed in 10% formalin for 72 h, then paraffin-embedded and cut into 4-µm-thick sections. Paraffin-embedded tissue sections were stained by anti-SPOCK2 antibody (abcam) according to the manufacturer's instructions. Following overnight incubation at 4 °C with the primary antibody, tissue sections were further stained with an appropriate horseradish peroxidase (HRP)-conjugated secondary antibody. Diaminobenzidine (DAB) staining was then performed on the sections, followed by rinsing with PBS, counterstaining with hematoxylin, and dehydration. Finally, all pictures were captured using a Nikon microscope.

2.13 Statistical analysis

Statistical analyses were performed using GraphPad Prism (version 5.0; La Jolla, CA). Data is expressed as mean ± SD. Comparisons between groups were performed using Student's t-test or one-way ANOVA (Tukey Kramer post hoc test). $P < 0.05$ was considered statistically significant.

3 Results

3.1 SPOCK2 is downregulated in human LUAD samples and cells

Analysis of UALCAN data showed that SPOCK2 expression was significantly decreased in LUAD specimens compared to normal tissues (Fig. 1A). Overall survival was analyzed using GEPIA. Patients with higher SPOCK2 expression levels exhibited significantly increased overall survival time compared to those with lower expression (Fig. 1B). Consistent with the findings from StarBase, immunohistochemistry (IHC) analysis revealed lower SPOCK2 protein levels in LUAD tissues compared to adjacent non-tumor tissues (Fig. 1C). Furthermore, western blot analysis demonstrated lower SPOCK2 protein expression in LUAD cell lines compared to normal human bronchial epithelial cells (BEAS-2B) (Fig. 1D). Collectively, these findings suggest that SPOCK2 is downregulated in LUAD and may exert an anti-tumor effect on disease progression.

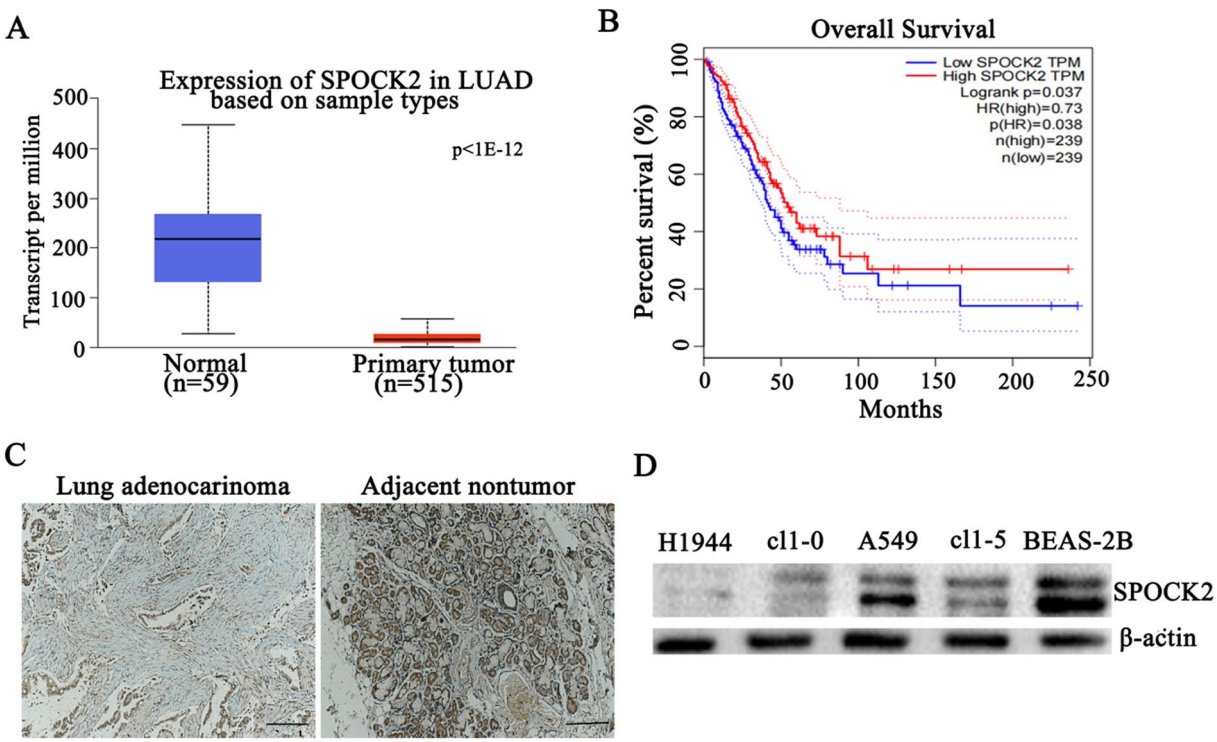

Fig. 1 SPOCK2 Downregulation in LUAD Tissues and Cell Lines. **A** UALCAN analysis: SPOCK2 mRNA expression is significantly lower in LUAD tissues compared to normal lung tissues (http://ualcan.path.uab.edu/index.html). **B** Overall survival analysis: Patients with higher SPOCK2 expression exhibit significantly increased overall survival compared to those with lower expression using the GEPIA dataset (p = 0.037). **C** SPOCK2 protein levels in tissues: Representative immunohistochemistry (IHC) staining for SPOCK2 in human LUAD tissues and adjacent non-tumor tissues (n = 10). The scale bars represent 200 µm. **D** SPOCK2 protein levels in cell lines: Western blot analysis of SPOCK2 protein expression in LUAD cell lines (H1944, Cl1-0, A549, Cl1-5) and normal human bronchial epithelial cells (BEAS-2B). *$P < 0.05$, **$P < 0.01$, ***$P < 0.001$

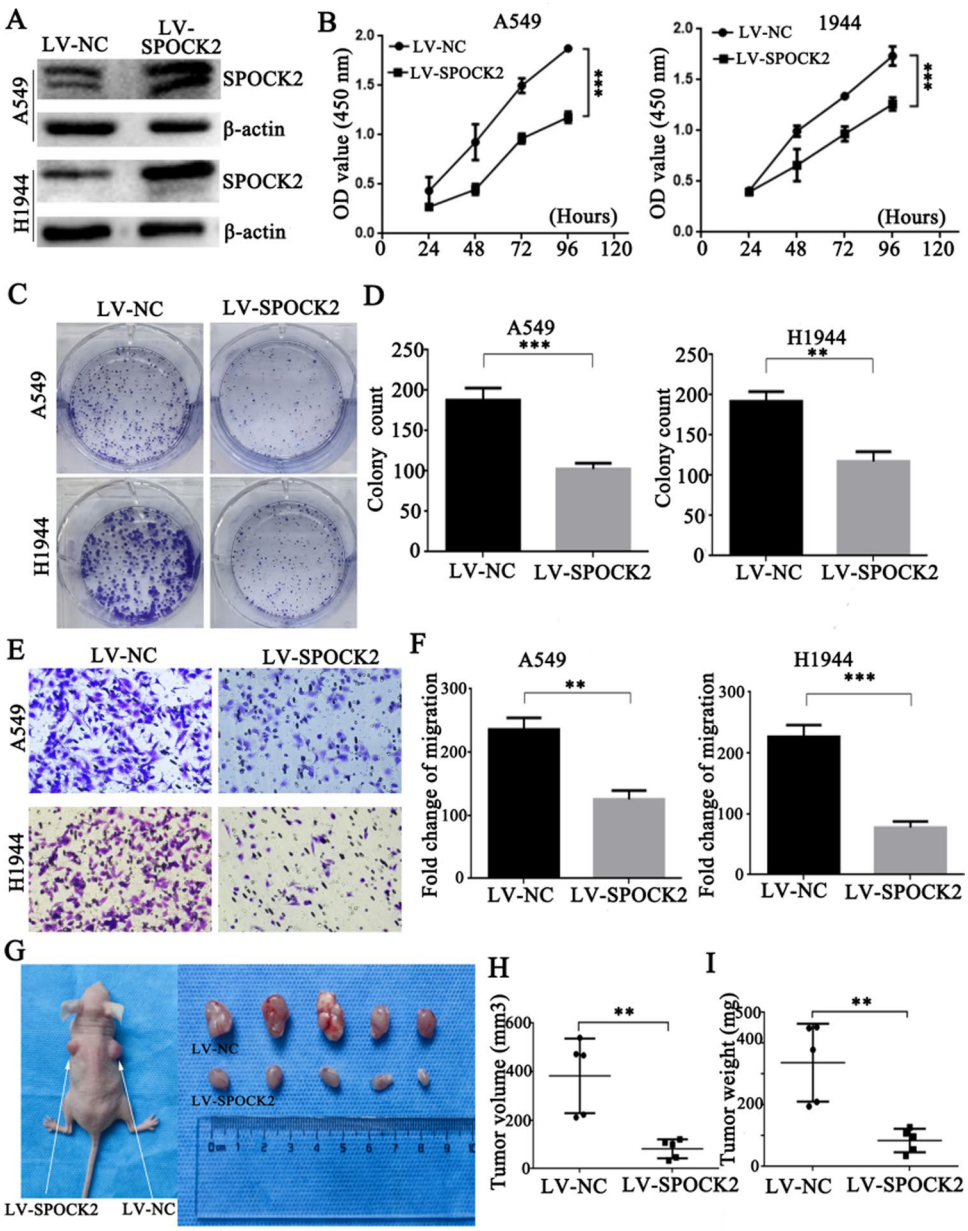

Fig. 2 SPOCK2 overexpression inhibits proliferation, migration and oncogenic transformation of LUAD cells. **A** Western blotting showed levels of SPOCK2 in lentivirus-infected A549 and H1944 cells. **B** CCK8 assays were performed on SPOCK2 overexpressing A549 and H1944 cells at 24, 48, 72 and 96 h to assess cell proliferation. **C**, **D** Colony formation assays were performed on SPOCK2 overexpressing A549 and H1944 cells, and representative micrographs of crystalline violet-stained cell colonies were shown, and the quantification was displayed (n = 3). **E**, **F** Transwell migration assays for cell migration assessment of SPOCK2 overexpressing A549 and H1944 cells were performed, the representative images (×200) were shown, the quantification was displayed (n = 3). **G**–**I** Nude mice xenograft model and the tumors were displayed, and tumor volume (**I**) and weight (**J**) were analysis. *$P < 0.05$, **$P < 0.01$, ***$P < 0.001$

3.2 SPOCK2 inhibits proliferation and migration of LUAD cell in vitro and overexpression of SPOCK2 suppresses tumor growth of LUAD in vivo

To assess the functional role of SPOCK2 in LUAD tumorigenesis, A549 and H1944 cells were transfected with lentiviral particles overexpressing SPOCK2 (LV-SPOCK2) (Fig. 2A). The CCK-8 assay showed that SPOCK2 overexpression significantly reduced LUAD cell proliferation (Fig. 2B). Consistent with this finding, the colony formation assay also demonstrated a significant decrease in colony number upon SPOCK2 overexpression in LUAD cells (Fig. 2C and D).

We further investigated the effect of SPOCK2 on LUAD cell migration using Transwell migration. The Transwell assay results demonstrated that SPOCK2 overexpression significantly inhibited LUAD cell migration (Fig. 2E and 2F). To assess the therapeutic potential of SPOCK2 in vivo, nude mice were subcutaneously injected with A549 cells stably transfected with either LV-SPOCK2 or a control lentivirus (LV-NC). All mice developed tumors at the injection site (Fig. 2G). Notably, the LV-SPOCK2 group exhibited significantly lower mean tumor volume and weight compared to the LV-NC group (Fig. 2H and I). Collectively, these findings suggest a tumor-suppressive role for SPOCK2 in LUAD progression.

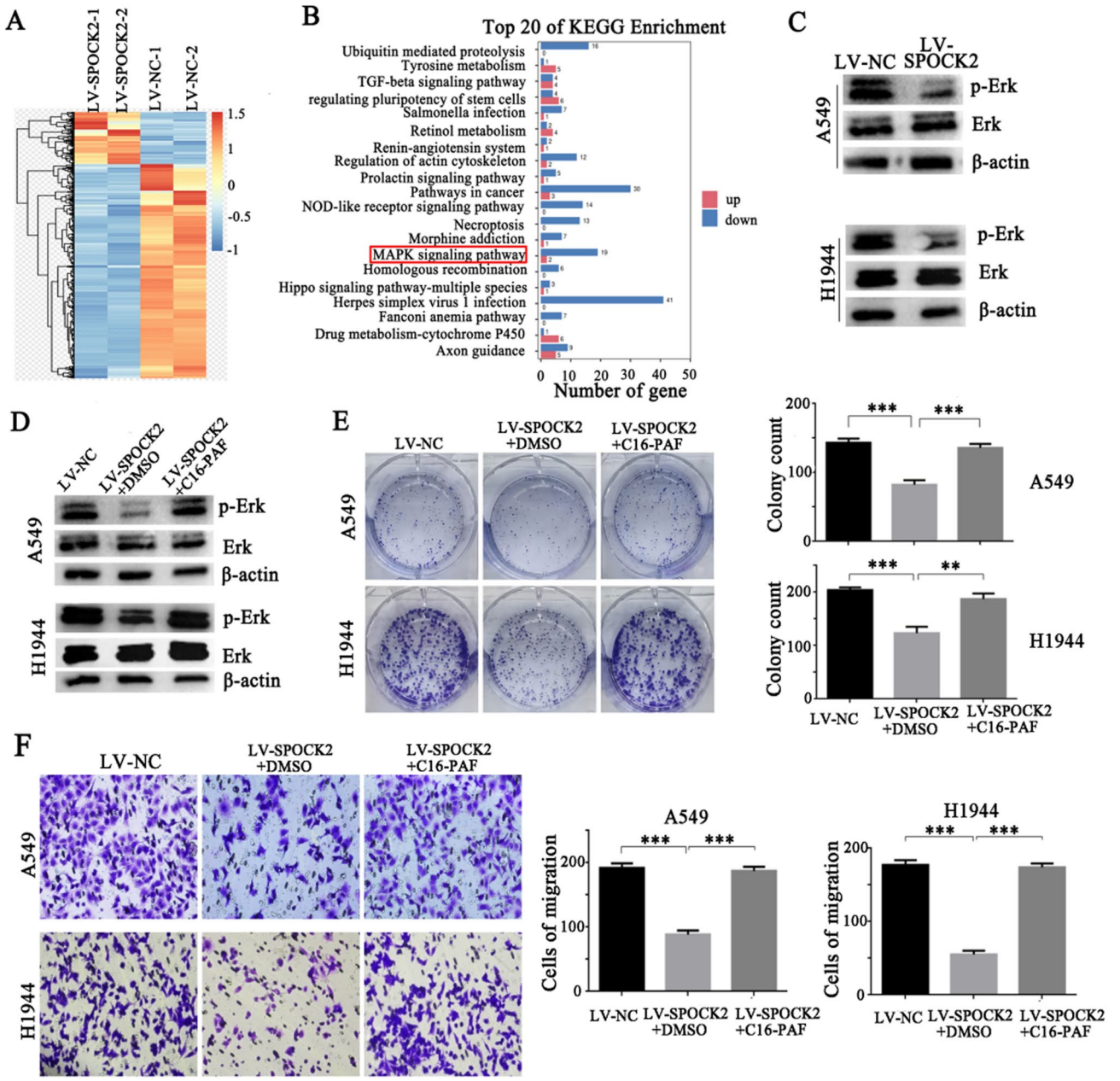

Fig. 3 SPOCK2 inhibits the MAPK signaling pathway. **A** Heat-map was constructed for DE mRNAs in LV-SPOCK2 vs Control. **B** KEGG analysis of the differentially up and down expressed genes between LV-SPOCK2 and LV-NC A549 cells. **C** The levels of p-Erk and Erk protein were measured by western blotting in SPOCK2-overexpression LUAD cells. **D** Activation efficiency of p-Erk protein in SPOCK2-overexpressing LUAD cells after C16-PAF treatment was assessed by western blotting. **E** Colony formation assay of SPOCK2-overexpression LUAD cells after MAPK activation (C16-PAF; left panel), and the quantification was shown (right panel; n = 3). **F** Transwell migration assay was used to assess the migration ability of SPOCK2-overexpressing LUAD cells after MAPK activation, the representative images (×200) were shown (left panel), and the quantification was displayed (right panel; n = 3). *$P < 0.05$, **$P < 0.01$, ***$P < 0.001$

3.3 SPOCK2 inhibits LUAD cell proliferation and migration by inactivating the MAPK pathway

To understand the mechanism by which SPOCK2 exerts its anti-tumor activity in LUAD, RNA transcriptome sequencing was performed on A549 cells transfected with either control or LV-SPOCK2 lentiviruses. Data were analyzed using the free online platform of LC-Bio Cloud Platform, and the comparison generated a heat map of differentially expressed genes (|log FC|> 1 and adjusted P-value < 0.05, Fig. 3A). Then, the Kyoto Encyclopedia of Genes and

Genomes enrichment analysis was also conducted using the free online platform of LC-Bio Cloud Platform. The analysis revealed enrichment of several pathways, including Herpes simplex virus 1 infection, pathways in cancer, the MAPK signaling pathway, and Ubiquitin-mediated proteolysis (Fig. 3B). Due to the high number of genes associated with the MAPK pathway and its established role in cancer, we focused on this pathway for further investigation [20]. Western blot analysis demonstrated that levels of phosphorylated Erk (p-Erk), a key protein in the MAPK pathway, were downregulated in SPOCK2-overexpressing cells compared to controls, while total Erk protein levels remained unchanged (Fig. 3C). Next, we activated the MAPK pathway in SPOCK2-overexpressing LUAD cells using C16-PAF, a known activator. C16-PAF treatment increased p-Erk protein levels in these cells (Fig. 3D). Furthermore, C16-PAF significantly reversed the inhibitory effects of SPOCK2 overexpression on LUAD cell proliferation and migration (Fig. 3E and F). These findings collectively suggest that the MAPK signaling pathway plays a critical role in SPOCK2-mediated tumor suppression in LUAD.

3.4 EVs derived from SPOCK2-modified HEK293T (SPOCK2-EVs) can effectively inhibit LUAD progression

EVs hold promise as ideal carriers for therapeutic agents. Their ability to deliver cargo such as chemotherapeutic drugs, siRNAs, and immunomodulators directly to cancer cells makes them particularly attractive. Notably, EVs exhibit stability under physiological and pathological conditions, and possess low immunogenicity [21]. To explore the potential clinical application of SPOCK2 in LUAD, we loaded SPOCK2 into EVs derived from HEK293T cells (SPOCK2-EVs) and investigated their effects on LUAD progression.

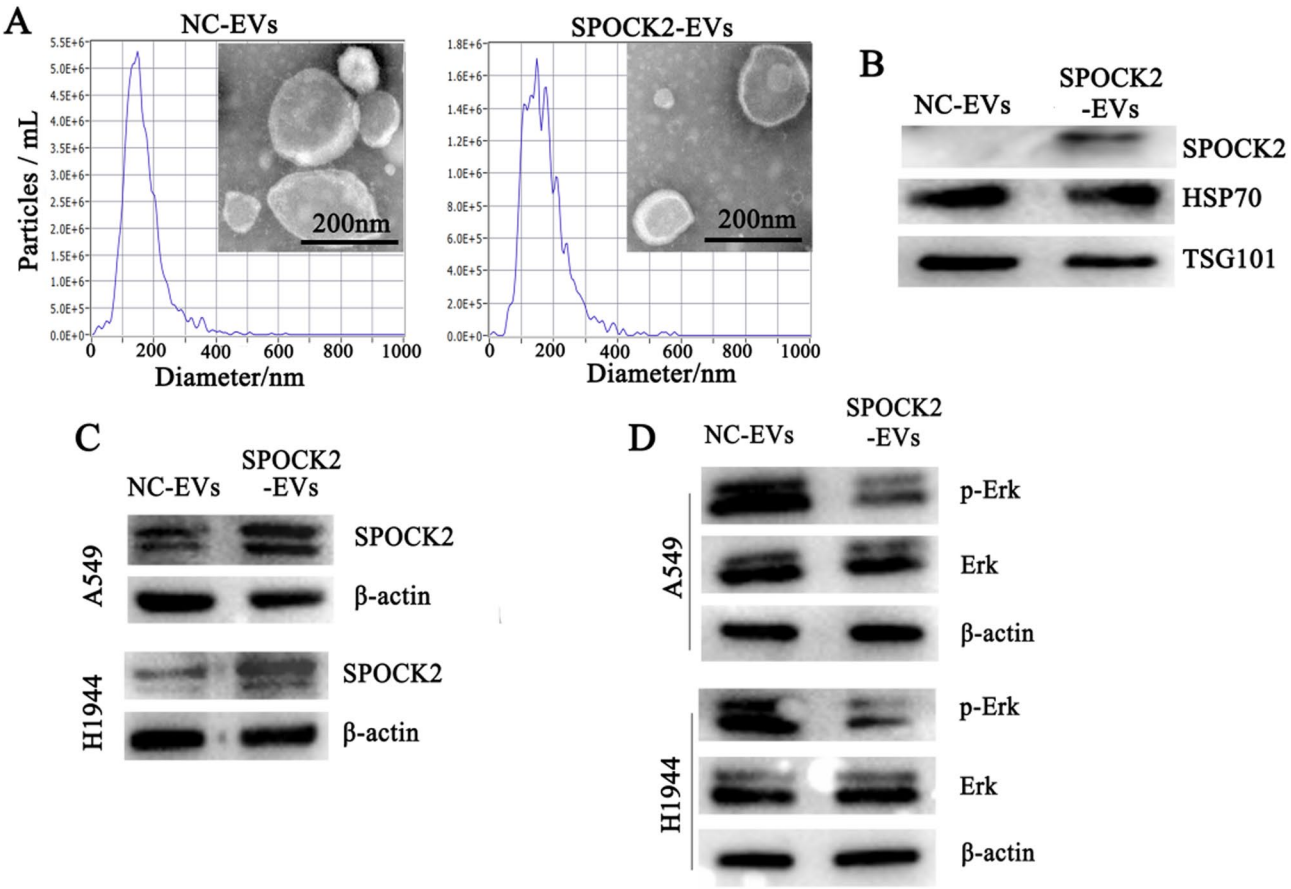

Fig. 4 EVs derived from SPOCK2-modified 293 T (SPOCK2-EVs) upregulate SPOCK2 expression in LUAD cells. **A** SPOCK2-EVs and NC-EVs were observed through a transmission electron microscope (Scale bars: 200 nm), and the size distributions of these EVs were examined by the Nanoparticle Tracking Analysis. **B** Western blot analysis of HSP70 and Tsg101 expression in SPOCK2-EVs and NC-EVs. Western blot analysis of SPOCK2 expression in SPOCK2-EVs and NC-EVs. **C** Western blot analysis of SPOCK2 expression in LUAD cells treated with SPOCK2-EVs and NC-EVs. **D** The levels of p-Erk and Erk protein in each group were examined by Western blot

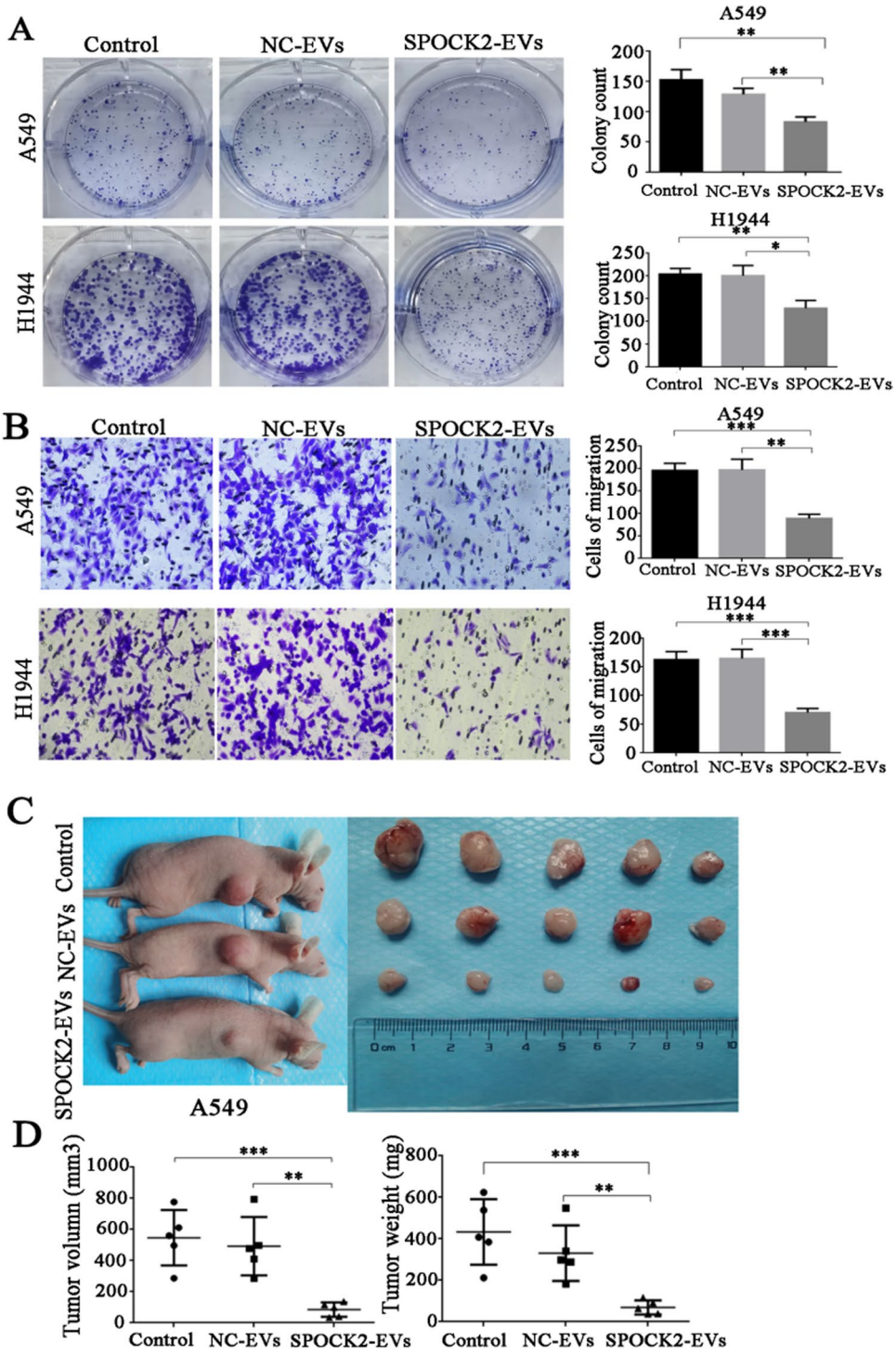

Fig. 5 SPOCK2-EVs inhibit LUAD progression in both vitro and vivo. **A** Colony formation assay (left panel) showed proliferation of LUAD cells in each group, the number of colonies was counted (right panel; n = 3). **B** Transwell migration assay (left panel) presented migration ability of each group. Magnification, ×200. Collective analysis of the migrating LUAD cell number treated with EVs (right panel; n = 3). **C** Subcutaneous tumors derived from A549 cells in nude mice 28 days after injection. **D** Statistical analysis of tumor volume and tumor weight in each A549 xenograft model group (n = 5). *$P < 0.05$; **$P < 0.01$, ***$P < 0.001$

Figure 4A shows that SPOCK2-EVs are spherical, membrane-bound particles with an average diameter of 171.9 nm. Consistent with established markers of EVs, they express heat shock protein 70 (HSP70) and tumor susceptibility gene 101 (Tsg101) [22]. Importantly, SPOCK2-EVs, but not NC-EVs, express SPOCK2, confirming successful loading into HEK293T-derived EVs (Fig. 4B). Furthermore, treatment with SPOCK2-EVs significantly increased SPOCK2 levels in LUAD cells compared to the NC-EV group (Fig. 4C). Additionally, SPOCK2-EV treatment resulted in reduced p-Erk protein levels compared to the NC-EV group (Fig. 4D).

Next, we assessed the effect of SPOCK2-EVs on LUAD cell proliferation and migration in vitro using colony formation and Transwell migration assays. As shown in Fig. 5A and B, SPOCK2-EVs significantly inhibited both proliferation

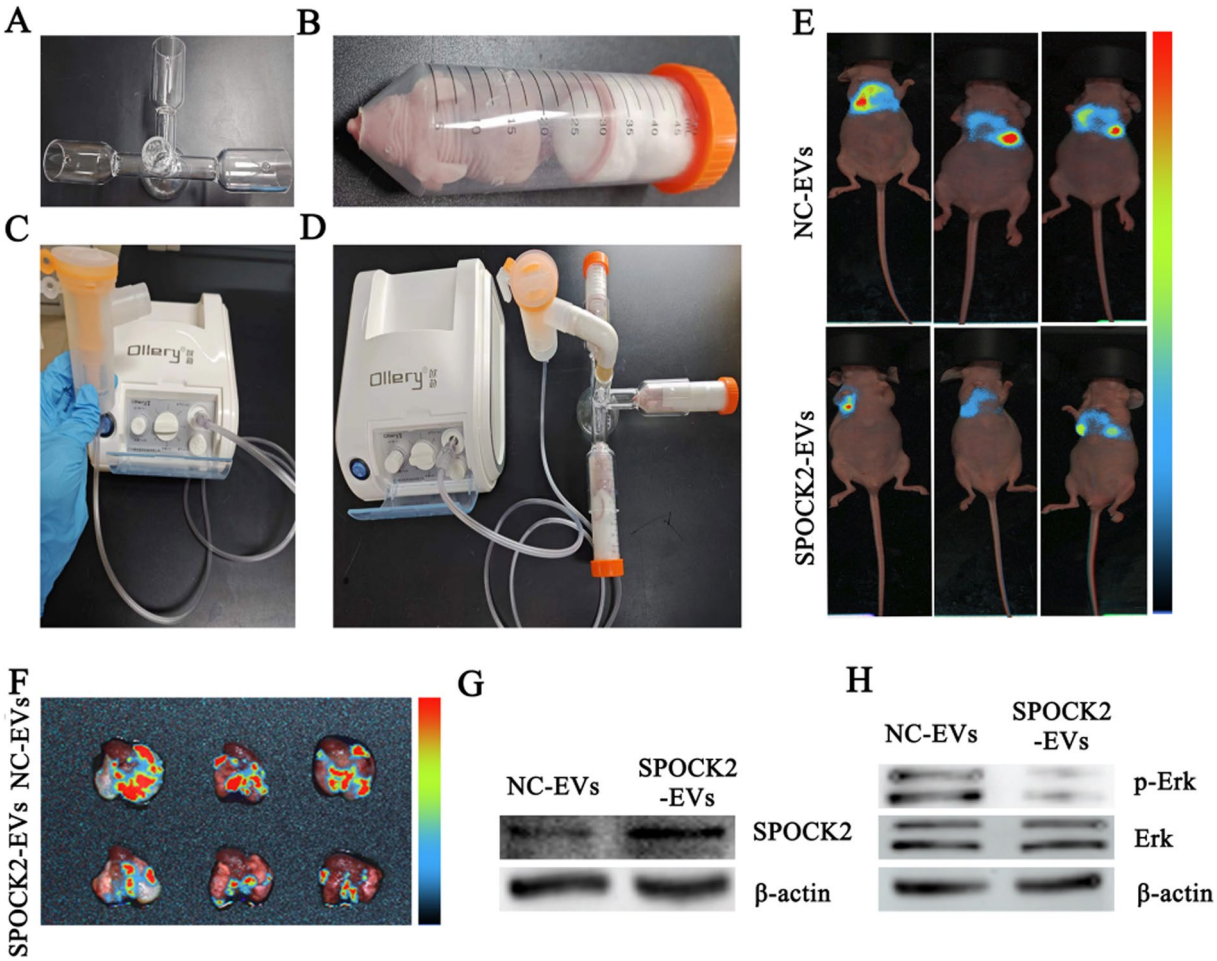

Fig. 6 Nebulized inhalation SPOCK2-EVs suppress LUAD growth in vivo. **A** Mouse three-way tube inhalation chamber describing aerosol flow patterns. This inhalation chamber consists of three parts (inlet tube, tee tube and base fixture). **B** Holding chamber for mouse. **C** Medical/domestic air compressors and nebulizer units. **D** Schematic diagram of mouse nebulized inhalation system. **E**, **F** The mice and their lungs investigated using the VILBER Fusion FX7 spectrum and the tumor images visualized by luciferase expression. The color scale represents intensity levels from blue (lowest) to red (highest). **G** Western blot analysis of SPOCK2 expression in lung tissues (lesion sites) treated with nebulized SPOCK2-EVs and NC-EVs. **H** The levels of p-Erk and Erk protein in each group were examined by Western blot

and migration of LUAD cells compared to the NC-EV group. To evaluate the in vivo efficacy of SPOCK2-EVs, we injected them directly into established A549 xenograft tumors in nude mice. Treatment with SPOCK2-EVs resulted in a significant reduction in tumor volume and weight compared to the NC-EV group (Fig. 5C and D).

3.5 Nebulized inhalation of SPOCK2-loaded EVs can significantly inhibit LUAD growth in mice

While our study demonstrated that intratumoral injection of SPOCK2-EVs significantly inhibited the growth of subcutaneous LUAD in nude mice, this method is clinically impractical. Therefore, we explored nebulized inhalation for SPOCK2-EV delivery, building upon our previous work [23]. Briefly, we utilized a medical/household air compressor and nebulizer to generate an aerosol of SPOCK2-EVs. This aerosol was then delivered to mice using a custom-designed and built mouse nebulizer inhaler device (Fig. 6A–D). Of note, fluorescence imaging revealed significantly attenuated fluorescence in the lungs of mice nebulized with SPOCK2-EVs compared to the NC-EV group (Fig. 6E and F). Additionally, Compared to the NC-EV group, mice treated with nebulized SPOCK2-EVs showed significantly increased SPOCK2 expression in lung tissues (lesion sites), along with markedly decreased p-Erk protein levels (Fig. 6G and H).

4 Discussion

Previous studies have reported conflicting roles for SPOCK2 in tumorigenesis, promoting growth in some cancers but inhibiting it in others [7, 11–13]. The function of SPOCK2 in LUAD remains poorly understood. Here, we demonstrate that SPOCK2 expression is downregulated in both LUAD tissues and cell lines compared to adjacent non-tumor tissues and normal bronchial epithelial cells, consistent with data from the UALCAN database. These findings suggest a potential tumor-suppressive role for SPOCK2 in LUAD. Furthermore, overexpression of SPOCK2 in LUAD cells significantly inhibited their proliferation and migration in vitro, and suppressed tumor growth in vivo using a subcutaneous xenograft model. Collectively, these results strongly suggest that SPOCK2 acts as a tumor suppressor in LUAD and may represent a promising therapeutic target.

The MAPK signaling pathway is a well-established contributor to tumor development [20]. Our combined RNA sequencing analysis and western blot assay confirmed that SPOCK2 negatively regulates p-Erk levels in LUAD cells. Although Fig. 1D shows a significant difference in SPOCK2 expression in the H1944 cell line compared to the control cell line (BEAS-2B), Fig. 3D shows that the change in p-Erk protein levels in response to SPOCK2 overexpression is less pronounced in H1944 compared to A549. The observed discrepancy may be attributed to intercellular heterogeneity among the tumor cell lines. Furthermore, activation of the MAPK pathway using a specific activator reversed the inhibitory effects of SPOCK2 overexpression on LUAD cell proliferation and migration. These findings strongly suggest that SPOCK2, at least partially, inhibits LUAD progression by suppressing the MAPK pathway. However, further investigation is needed to elucidate the precise mechanism by which SPOCK2 exerts its inhibitory effect on this pathway in LUAD. Our findings demonstrate that SPOCK2 functions as a tumor suppressor by inhibiting proliferation and migration of LUAD cells. However, efficient delivery of SPOCK2 to the tumor site remains a critical hurdle for clinical translation. Our previous work [24] showed that Yes Kinase-associated Protein (YAP) can be transferred from LUAD cells to endothelial cells via extracellular vesicles (EVs). This raises the intriguing possibility of utilizing EVs as a delivery system to transport SPOCK2 to lung cancer cells in vivo, potentially exerting a therapeutic effect.

Extracellular vesicles (EVs) are nanoscale membrane-bound vesicles released by various cell types [25]. Their unique properties, including minimal immunogenicity, long-term stability in storage, and resistance to vascular embolism, make them ideal candidates for "cell-free" therapeutic applications [26]. Notably, EVs have shown promise in lung cancer treatment. For instance, A.K. Agrawal et al. (2017) demonstrated that milk-derived EVs loaded with paclitaxel (bmExo-PAC) significantly inhibited tumor growth in a mouse model of lung cancer upon oral administration [27]. Similarly, Huang Nie et al. (2019) reported that tail vein injection of EVs derived from breast cancer cells (MDA-MB-231) carrying miRNA-126 effectively suppressed lung cancer metastasis [28]. EVs possess the capacity to deliver a variety of therapeutic agents, including chemotherapeutic drugs, siRNAs, and immunomodulators, directly into cancer cells. Furthermore, their stability under physiological and pathological conditions, coupled with low immunogenicity, makes them advantageous compared to other nanocarriers [21]. Utilizing EVs as biovectors for delivering tumor suppressor genes represents a novel and promising strategy for cancer treatment [29, 30].

To minimize the influence of confounding factors, we employed HEK293T cells as the source for EVs. These cells significantly enriched SPOCK2 levels within the EVs upon SPOCK2 overexpression. Moreover, intratumoral injection of SPOCK2-EVs resulted in a significant reduction in LUAD growth. These findings suggest that loading SPOCK2 into EVs represents a promising approach for clinical translation. While directly injecting EVs into tumors holds promise, it presents challenges for internal organs [31]. Conventional delivery methods for lung cancer treatment, such as oral or intravenous injection, can lead to significant waste of EVs and impose a burden on the body's metabolism (e.g., liver). Additionally, these methods carry risks of systemic or localized infections and systemic side effects, potentially compromising patient compliance [31]. Therefore, safer and more effective delivery strategies are needed. Inhalation therapy, a cornerstone treatment for respiratory diseases [32–34], offers a non-invasive route for localized drug delivery to the lungs [35]. This approach achieves superior targeting compared to other methods [36, 37].

Compared to other administration routes, inhalation drug delivery offers several advantages, including reduced dosage requirements, minimized systemic toxicity, and improved patient compliance [38]. Notably, a recent study by Liu et al. (2024) demonstrated that inhaled EVs loaded with IL-12 mRNA effectively treated lung cancer in mice, inducing both local and systemic anti-tumor immune responses [39]. Building upon this research and our previous work on nebulized drug delivery [23], we investigated the efficacy of nebulized SPOCK2-EVs for LUAD treatment. Consistent with our findings from intratumoral injection, nebulized inhalation of SPOCK2-EVs resulted in significant inhibition of LUAD growth.

In our preliminary studies, we have observed that nebulized EVs can bind to bronchial epithelial cells [40]. LUAD is a tumor originating from the bronchial mucosal epithelium. Therefore, the inhibitory effect of nebulized SPOCK2-EVs on LUAD growth may directly result from tumor cell uptake of EVs. This suggests that compared to peripheral-type lung cancer, central-type lung cancer might demonstrate better therapeutic efficacy with nebulized EV treatment due to the larger contact area between EVs and the tumor. However, we cannot exclude the possibility of indirect mechanisms, as recent studies have revealed that nebulized EVs can interact not only with epithelial cells but also with macrophages [41].

Our findings demonstrate that: (1) SPOCK2-EVs derived from HEK293T cells efficiently deliver SPOCK2 to LUAD cells, leading to increased SPOCK2 protein levels and suppression of the MAPK pathway. (2) Treatment with SPOCK2-EVs significantly inhibits proliferation and migration of LUAD cells in vitro. (3) SPOCK2-EVs effectively suppress LUAD tumor growth in BALB/c nude mice, as demonstrated by both intratumoral injection and nebulized inhalation delivery methods. In conclusion, these results strongly suggest that SPOCK2 released by HEK293T-EVs can effectively inhibit LUAD tumor growth and hold promise for future clinical translation in cancer therapy.

This study does have a number of limitations: (1) It remains unclear whether the inhibition of LUAD growth by nebulized inhalation of SPOCK2-EVs is due to direct uptake of EVs by tumor cells or is indirectly mediated. A detailed investigation into which specific cell types interact with nebulized EVs is currently lacking. (2) It is not clear what is the optimal amount of SPOCK2-EVs through nebulized inhalation. (3) The safety of nebulized inhalation needs further evaluation.

5 Conclusions

To our knowledge, this study provides the first evidence that SPOCK2 functions as a regulator of LUAD cell proliferation and migration by suppressing the MAPK signaling pathway. Furthermore, we demonstrate that SPOCK2-EVs effectively inhibit LUAD growth. We also propose and validate a novel approach for LUAD treatment: nebulized inhalation of SPOCK2-EVs. This method demonstrably inhibits LUAD growth, suggesting potential for SPOCK2-EVs as a therapeutic strategy for LUAD patients and potentially other diseases associated with SPOCK2 abnormalities.

Acknowledgements Not applicable.

Author contributions Y.W. and JH. J. designed the study and wrote the manuscript. Y.W. and LY. D. designed the methodology. Y.W., NN. L., CQ. X. and J.W. performed experiments and collected data. Y.W. and S.Y. analyzed data. S.Y. and JH. J. interpreted data, provided administrative, technical, or material support and revised the manuscript. All authors have read and approved the final manuscript.

Funding This work was supported by Soochow University Start-up Fund, the Priority Academic Program Development of the Jiangsu Higher Education Institutes (PAPD), Jiangsu Science and Technology Plan Funding (BX2022023), the Jiangsu Shuangchuang Boshi Funding (JSSCBS20210697), Suzhou Project Funding (SKY2021026), Suzhou Medical Innovation Funding (SKJY2021141).

Data availability The datasets generated and analyzed during the current study are available from the corresponding author on reasonable request. Data requests can be made via this email: liyangdong@ujs.edu.cn.

Declarations

Ethics approval and consent to participate All samples were collected after obtaining patients' written informed consent. LUAD and normal lung tissue specimens were obtained from informed, consenting LUAD patients at the Affiliated Huai'an Hospital of Xuzhou Medical University. All study protocols were approved by the Ethics Committee of the Affiliated Huai'an Hospital of Xuzhou Medical University (HEYLL202302), which abides by the Helsinki Declaration on ethical principles for medical research. Experiments about animals were performed in accordance with the guidelines of the National Institutes of Health Guide for the Care and Use of Laboratory Animals. Study protocols were approved by the Ethics Committee of Soochow University (SUDA20230428A06).

Competing interests The authors declare no competing interests.

References

1. Forde PM, Spicer J, Lu S, et al. neoadjuvant nivolumab plus chemotherapy in resectable lung cancer. New Engl J Med. 2022;386(21):1973–85.
2. Chen J, Yang H, Teo A, et al. Genomic landscape of lung adenocarcinoma in East Asians. Nat Genet. 2020;52(2):177–86.
3. Hirsch FR, Scagliotti GV, Mulshine JL, et al. Lung cancer: current therapies and new targeted treatments. Lancet. 2017;389(10066):299–311.
4. Siegel RL, Miller KD, Fuchs HE, Jemal A. Cancer statistics, 2021. CA-Cancer J Clin. 2021;71(1):7–33.
5. Saynak M, Veeramachaneni NK, Hubbs JL, et al. Local failure after complete resection of N0–1 non-small cell lung cancer. Lung Cancer. 2011;71(2):156–65.
6. Mouw JK, Ou G, Weaver VM. Extracellular matrix assembly: a multiscale deconstruction. Nat Rev Mol Cell Bio. 2014;15(12):771–85.
7. Liu G, Ren F, Song Y. Upregulation of SPOCK2 inhibits the invasion and migration of prostate cancer cells by regulating the MT1-MMP/MMP2 pathway. PeerJ. 2019;7: e7163.
8. Vancza L, Karaszi K, Peterfia B, et al. SPOCK1 promotes the development of hepatocellular carcinoma. Front Oncol. 2022;12: 819883.
9. Cui X, Wang Y, Lan W, et al. SPOCK1 promotes metastasis in pancreatic cancer via NF-kappaB-dependent epithelial-mesenchymal transition by interacting with IkappaB-alpha. Cell Oncol. 2022;45(1):69–84.
10. Barrera-Ocampo A, Arlt S, Matschke J, et al. Amyloid-beta precursor protein modulates the sorting of testican-1 and contributes to its accumulation in brain tissue and cerebrospinal fluid from patients with Alzheimer disease. J Neuropath Exp Neur. 2016;75(9):903–16.
11. Aghamaliyev U, Su K, Weniger M, et al. SPOCK2 gene expression is downregulated in pancreatic ductal adenocarcinoma cells and correlates with prognosis of patients with pancreatic cancer. J Cancer Res Clin. 2023;149(11):9191–200.
12. Ren F, Wang D, Wang Y, Chen P, Guo C. SPOCK2 affects the biological behavior of endometrial cancer cells by regulation of MT1-MMP and MMP2. Reprod Sci. 2020;27(7):1391–9.
13. Lou W, Ding B, Zhong G, Du C, Fan W, Fu P. Dysregulation of pseudogene/lncRNA-hsa-miR-363-3p-SPOCK2 pathway fuels stage progression of ovarian cancer. Aging (Albany NY). 2019;11(23):11416–39.
14. Zhao J, Cheng M, Gai J, Zhang R, Du T, Li Q. SPOCK2 serves as a potential prognostic marker and correlates with immune infiltration in lung adenocarcinoma. Front Genet. 2020;11: 588499.
15. Liu Y, Fan X, Jiang C, Xu S. SPOCK2 and SPRED1 function downstream of EZH2 to impede the malignant progression of lung adenocarcinoma in vitro and in vivo. Hum Cell. 2023;36(2):812–21.
16. Chandrashekar DS, Bashel B, Balasubramanya SAH, et al. UALCAN: a portal for facilitating tumor subgroup gene expression and survival analyses. Neoplasia. 2017;19(8):649–58.
17. Tang Z, Li C, Kang B, et al. GEPIA: a web server for cancer and normal gene expression profiling and interactive analyses. Nucleic Acids Res. 2017;45(W1):W98–102.
18. Bruno S, Collino F, Deregibus MC, Grange C, Tetta C, Camussi G. Microvesicles derived from human bone marrow mesenchymal stem cells inhibit tumor growth. Stem Cells Dev. 2013;22(5):758–71.
19. Lang FM, Hossain A, Gumin J, et al. Mesenchymal stem cells as natural biofactories for exosomes carrying miR-124a in the treatment of gliomas. Neuro Oncol. 2018;20(3):380–90.
20. Yaeger R, Corcoran RB. Targeting alterations in the RAF-MEK pathway. Cancer Discov. 2019;9(3):329–41.
21. Saviana M, Romano G, Le P, Acunzo M, Nana-Sinkam P. Extracellular vesicles in lung cancer metastasis and their clinical applications. Cancers. 2021;13(22):5633.
22. Thery C, Witwer KW, Aikawa E, et al. Minimal information for studies of extracellular vesicles 2018 (MISEV2018): a position statement of the International Society for extracellular vesicles and update of the MISEV2014 guidelines. J Extracell Vesicles. 2018;7(1):1535750.
23. Xu X, Wang Y, Luo X, et al. A non-invasive strategy for suppressing asthmatic airway inflammation and remodeling: inhalation of nebulized hypoxic hUCMSC-derived extracellular vesicles. Front Immunol. 2023;14:1150971.
24. Wang Y, Dong L, Zhong H, et al. Extracellular vesicles (EVs) from lung adenocarcinoma cells promote human umbilical vein endothelial cell (HUVEC) angiogenesis through yes kinase-associated protein (YAP) transport. Int J Biol Sci. 2019;15(10):2110–8.
25. van Niel G, D'Angelo G, Raposo G. Shedding light on the cell biology of extracellular vesicles. Nat Rev Mol Cell Bio. 2018;19(4):213–28.
26. Jafarinia M, Alsahebfosoul F, Salehi H, Eskandari N, Ganjalikhani-Hakemi M. Mesenchymal stem cell-derived extracellular vesicles: a novel cell-free therapy. Immunol Invest. 2020;49(7):758–80.
27. Agrawal AK, Aqil F, Jeyabalan J, et al. Milk-derived exosomes for oral delivery of paclitaxel. Nanomedicine. 2017;13(5):1627–36.
28. Nie H, Xie X, Zhang D, et al. Use of lung-specific exosomes for miRNA-126 delivery in non-small cell lung cancer. Nanoscale. 2020;12(2):877–87.
29. Kamerkar S, LeBleu VS, Sugimoto H, et al. Exosomes facilitate therapeutic targeting of oncogenic KRAS in pancreatic cancer. Nature. 2017;546(7659):498–503.
30. Winkle M, El-Daly SM, Fabbri M, Calin GA. Noncoding RNA therapeutics - challenges and potential solutions. Nat Rev Drug Discov. 2021;20(8):629–51.
31. Qiu N, Wang G, Wang J, et al. Tumor-associated macrophage and tumor-cell dually transfecting polyplexes for efficient interleukin-12 cancer gene therapy. Adv Mater. 2021;33(2): e2006189.
32. Lundback B, Backman H, Lotvall J, Ronmark E. Is asthma prevalence still increasing? Expert Rev Resp Med. 2016;10(1):39–51.
33. Daniels T, Mills N, Whitaker P. Nebuliser systems for drug delivery in cystic fibrosis. Cochrane DB Syst Rev. 2013;4:D7639.
34. Hickey AJ. Emerging trends in inhaled drug delivery. Adv Drug Deliver Rev. 2020;157:63–70.
35. Dinh PC, Paudel D, Brochu H, et al. Inhalation of lung spheroid cell secretome and exosomes promotes lung repair in pulmonary fibrosis. Nat Commun. 2020;11(1):1064.
36. Li Y, Su Z, Zhao W, et al. Multifunctional oncolytic nanoparticles deliver self-replicating IL-12 RNA to eliminate established tumors and prime systemic immunity. Nat Cancer. 2020;1(9):882–93.
37. Muller JM, Wissemann J, Meli ML, et al. In vivo induction of interferon gamma expression in grey horses with metastatic melanoma resulting from direct injection of plasmid DNA coding for equine interleukin 12. Schweiz Arch Tierh. 2011;153(11):509–13.

38. Gupta C, Jaipuria A, Gupta N. Inhalable formulations to treat non-small cell lung cancer (NSCLC): recent therapies and developments. Pharmaceutics. 2022;15(1):139.
39. Liu M, Hu S, Yan N, Popowski KD, Cheng K. Inhalable extracellular vesicle delivery of IL-12 mRNA to treat lung cancer and promote systemic immunity. Nat Nanotechnol. 2024;19:565–75.
40. Luo X, Wang Y, Mao Y, et al. Nebulization of hypoxic hUCMSC-EVs attenuates airway epithelial barrier defects in chronic asthma mice by transferring CAV-1. Int J Nanomed. 2024;19:10941–59.
41. Han Y, Zhu Y, Youngblood HA, et al. Nebulization of extracellular vesicles: a promising small RNA delivery approach for lung diseases. J Control Release. 2022;352:556–69.